Dynamics of Katabatic Winds in Colorado's Brush Creek Valley

I. VERGEINER AND E. DREISEITL

Institute for Meteorology and Geophysics, University of Innsbruck, Austria

C. DAVID WHITEMAN*

Institute for Meteorology, University of Munich, Federal Republic of Germany

(Manuscript received 11 February 1986, in final form 5 August 1986)

ABSTRACT

A method is proposed to evaluate the coupled mass, momentum and thermal energy budget equations for a deep valley under two-dimensional, steady-state flow conditions. The method requires the temperature, down-valley wind and valley width fields to be approximated by simple analytical functions. The vertical velocity field is calculated using the mass continuity equation. Advection terms in the momentum and energy equations are then calculated using finite differences computed on a vertical two-dimensional grid that runs down the valley's axis. The pressure gradient term in the momentum equation is calculated from the temperature field by means of the hydrostatic equation. The friction term is then calculated as a residual in the x-momentum equation, and the diabatic cooling term is calculated as a residual in the thermal energy budget equation.

The method is applied to data from an 8-km-long segment of Colorado's Brush Creek Valley on the night of 30–31 July 1982. Pressure decreased with distance down the valley on horizontal surfaces, with peak horizontal pressure gradients of 0.04 hPa km^{-1}. The valley mass budget indicated that subsidence was required in the valley to support calculated mean along-valley mass flux divergence. Peak subsidence rates on the order of 0.10 m s^{-1} were calculated. Subsiding motions in the valley produced negative vertical down-valley momentum fluxes in the upper valley atmosphere, but produced positive down-valley momentum fluxes below the level of the jet. Friction, calculated as a residual in the x-momentum equation, was negative, as expected on physical grounds, and attained reasonable quantitative values.

The strong subsidence field in the stable valley atmosphere produced subsidence warming that was only partly counteracted by down-valley cold air advection. Strong diabatic cooling was therefore required in order to account for the weak net cooling of the valley atmosphere during the nighttime period when tethered balloon observations were made.

1. Introduction

Whiteman and Barr (1986, hereafter referred to as WB) recently published an analysis of the atmospheric mass fluxes on the clear night of 30–31 July 1982 in an 8-km segment of Colorado's Brush Creek Valley. Their analysis was based on tethered balloon data collected as part of the U.S. Department of Energy's Atmospheric Studies in Complex Terrain (ASCOT) Program. Whiteman and Barr's analysis represents an attempt to evaluate the fluxes of mass into and out of the valley segment using the mass continuity equation under the assumption that the wind field is uniform across the valley. A key finding of the paper was that a strong subsidence field was required in the valley in order to satisfy the mean along-valley mass flux divergence that occurred during a 7-h nocturnal steady-state period. This mean subsidence field was expected to have a strong influence on the valley momentum and thermal energy budgets.

In this paper we propose a method by which to evaluate individual terms of the coupled mass, momentum and thermal energy budgets of a valley under conditions where the wind field is steady-state and atmospheric variables can be considered to be uniform in the cross-valley direction. We then present a preliminary evaluation of the method using data from the 1982 ASCOT experiment. In this attempt we begin with the WB wind speed and mass budget data and add some preliminary information on the along-valley and vertical temperature structure to try to derive mutually consistent fields of horizontal and vertical velocities, momentum advection, temperature advection and pressure. The friction term in the momentum equation and the diabatic cooling term in the thermal energy budget are determined as residuals.

2. Assumptions and analysis method

Our main assumption is that all fields may be considered uniform in the cross-valley direction y, such that all information is contained in two-dimensional x (along-valley direction)–z (vertical) sections. Under

* Permanent affiliation: Pacific Northwest Laboratory, Richland, Washington.

© 1987 American Meteorological Society

Unauthenticated | Downloaded 11/30/22 12:29 AM UTC

the assumption of steady-state winds and atmospheric variables uniform in the cross-valley direction, we wish to evaluate individual terms in the horizontal momentum and thermodynamic energy equations. This evaluation will be accomplished by defining a two-dimensional along-valley coordinate system, approximating the two-dimensional wind and temperature fields and the valley width with simple analytical functions, and evaluating individual terms of the momentum and thermodynamic energy equations on the coordinate grid using the analytical functions. This method has an advantage over methods that rely on the separate calculation of mass, momentum and thermal energy budgets since the analytical functions can be adjusted easily to determine how a small change in the wind, temperature or topography fields will affect all of the coupled equations.

a. Coordinate system

We define two coordinate systems (Fig. 1) for an along-valley section, with both coordinate systems having their origin on the valley floor at the upper end of the valley section. The first coordinate system follows the valley floor (ξ–ζ), and the other has a horizontal x-axis (x–z). Application of this coordinate system to the Brush Creek Valley observations, to be discussed later, will be made for an (x–z)-grid resolution of $\Delta x = 1$ km and $\Delta z = 15$ m. Coordinate transformations, then, are given as follows:

$$\left.\begin{aligned}\xi &= x\cos\alpha - z\sin\alpha\\ \zeta &= x\sin\alpha + z\cos\alpha\end{aligned}\right\}, \tag{1}$$

where

$$\alpha = 0.86^\circ \quad (\tan\alpha = 120\text{ m}/8000\text{ m}).$$

b. System of equations

We begin by assuming that the along-valley wind and temperature fields in the valley segment can be approximated closely by analytical functions $V(\xi, \zeta)$ and $T(\xi, \zeta)$ and that the distance from sidewall to sidewall on a valley cross section $\Delta y(\xi, \zeta)$ can also be approximated by a simple analytical function.

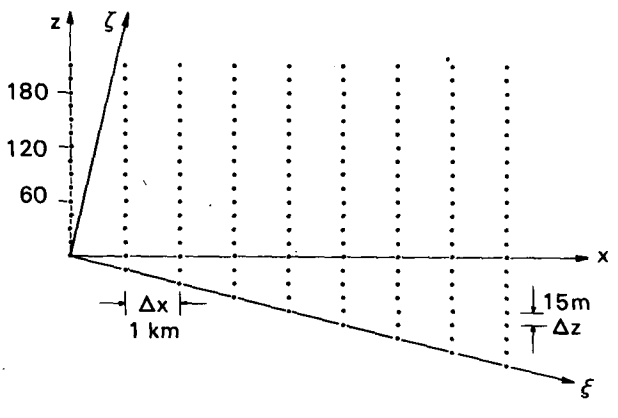

FIG. 1. Coordinate systems and the numerical grid.

Now a streamfunction ψ may be defined, which equals the cumulative along-valley volume flux in m^3 s^{-1} up to height ζ:

$$\psi = \int_0^{\zeta} V(\zeta')\Delta y(\zeta')d\zeta'. \tag{2}$$

The vertical motion field can then be calculated in (ξ–ζ) coordinates as

$$w^* = -\frac{1}{\Delta y}\frac{\partial\psi}{\partial\xi},$$

or the down-valley and vertical motion fields can be calculated in (x–z) coordinates as

$$\left.\begin{aligned}u &= \frac{1}{\Delta y}\frac{\partial\psi}{\partial z}\\ w &= -\frac{1}{\Delta y}\frac{\partial\psi}{\partial x}\end{aligned}\right\}. \tag{3}$$

The valley pressure field can be calculated from the valley temperature field using the hydrostatic equation and the boundary condition that the horizontal pressure gradient is negligible at ridgetop level. We wish to do these calculations using potential temperature, where, to a good approximation:

$$\theta = T + \frac{Z(m)}{100}. \tag{4}$$

The hydrostatic equation then becomes

$$\frac{1}{\rho_0}\frac{\partial p'}{\partial z} = \frac{g}{\theta_0}\theta', \tag{5}$$

where potential temperature and pressure have been linearized as follows:

$$\left.\begin{aligned}\theta &\equiv \bar{\theta}(z) + \theta'(x,z)\\ p &\equiv \bar{p}(z) + p'(x,z)\end{aligned}\right\}.$$

By integration downward over a height interval H we obtain

$$(p'_1 - p'_2) = \rho_0 H\frac{g}{\theta_0}(\bar{\theta}'_2 - \bar{\theta}'_1). \tag{6}$$

Subscripts 1 and 2 refer to the upstream and downstream valley ends, and the overbars are vertical averages.

Arbitrarily setting θ ($\xi = 8$ km) $\equiv \bar{\theta}(z)$, the potential temperature deviation θ' is calculated and the pressure field p' is obtained by integrating the hydrostatic equation [Eq. (5)] downward, assuming $p' \approx 0$ near ridgetop level.

Naturally, we expect pressure to decrease in the down-valley direction in the problem at hand, since it is this pressure gradient $\partial p'/\partial x$ that drives the katabatic wind.

Unauthenticated | Downloaded 11/30/22 12:29 AM UTC

For quasi-two-dimensional flow the momentum equation in the x-direction is written:

$$\frac{\partial u}{\partial t} = -\left[u\frac{\partial u}{\partial x} + w\frac{\partial u}{\partial z}\right] - \frac{1}{\rho}\frac{\partial p'}{\partial x} + \text{friction}. \quad (7)$$

momentum advection; pressure gradient

The pressure gradient term is expected to be positive everywhere and friction negative. The advection and pressure gradient terms in this equation can be evaluated at grid points using finite differencing with the use of Eqs. (3) and (5). Under the assumed steady-state conditions, a balance is obtained between momentum advection, pressure gradient and friction. Friction is determined as a residual in the steady-state x-momentum equation.

The energy balance at a point in the valley segment under conditions of two-dimensional, stationary flow is

$$\frac{\partial \theta}{\partial t} = -\left[u\frac{\partial \theta}{\partial x} + w\frac{\partial \theta}{\partial z}\right] + D. \quad (8)$$

storage; temperature advection; diabatic heating or cooling rate

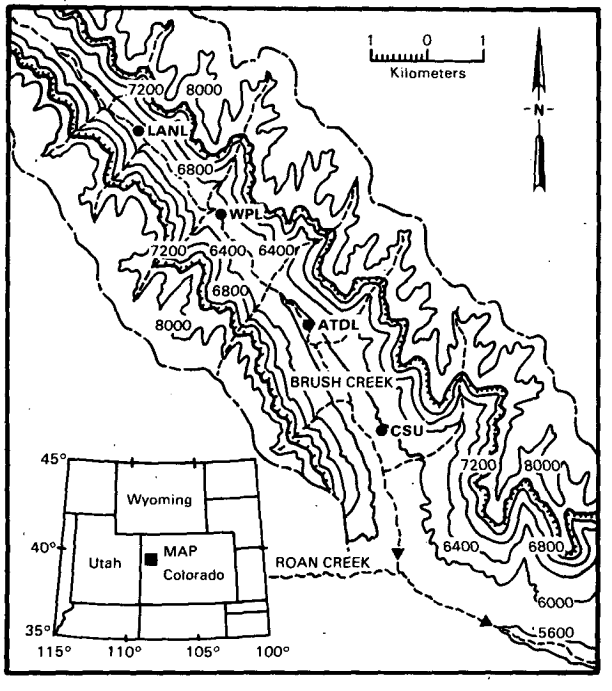

FIG. 2. Relief of the lowest 12 km of Colorado's Brush Creek Valley. The outline of the valley drainage area and the location of the valley "rim" are shown. Dots indicate the locations of tethersonde sites. Site names indicate the laboratories that collected the data. LANL is the Los Alamos National Laboratory, WPL is the Wave Propagation Laboratory of the National Oceanic and Atmospheric Administration (NOAA), ATDL is NOAA's Atmospheric Turbulence and Diffusion Laboratory, and CSU is Colorado State University.

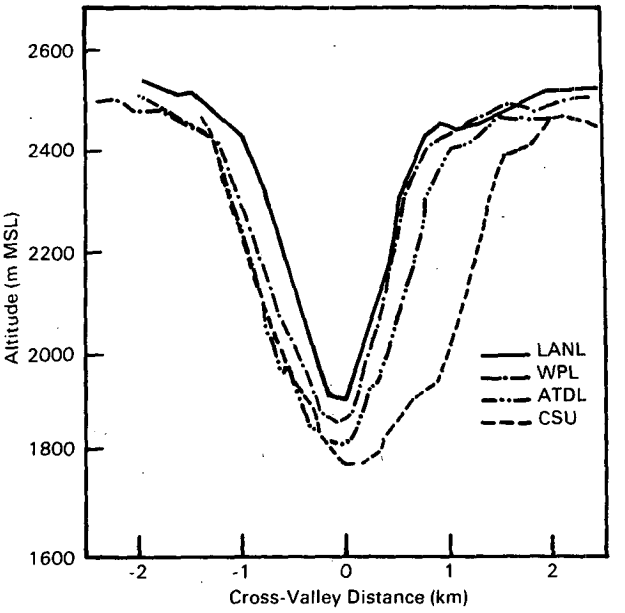

FIG. 3. Cross sections of the Brush Creek Valley at four tethered balloon sites.

By now, we have everything needed to compute the advection terms in this equation. The storage term can be computed from potential temperature differences between successive soundings. Thus we can determine the diabatic heating or cooling rates in the valley as a residual.

3. Application to the 1982 Brush Valley data

As the next step in our analysis we wish to use the 30–31 July 1982 Brush Creek Valley data to perform a test of the method.

The Brush Creek Valley is a 650-m deep valley carved into the Roan Plateau of western Colorado (Fig. 2). In 1982 ASCOT field measurements were taken along an approximately 8-km-long segment at the lower end of the valley. These measurements were essentially restricted to the narrow part of the valley below a prominent valley rim that lies at about 2377 m MSL (7800 ft) at both the upstream and downstream ends of the valley. The valley floor slope is about 120 m in the 8-km valley segment, with valley floor elevations varying from 1800 to 1920 m MSL. Topographic cross sections of the valley at various points along the valley's axis are shown in Fig. 3.

Wind conditions in the valley were reported by WB to be more or less stationary between 2200 and 0500 LST. Our considerations apply to this quasi-stationary state. Down-valley wind speed profiles at several locations along the axis of the valley (Fig. 4) exhibited "jet" profiles in which maximum windspeeds reached 7 m s^{-1} only 90–150 m above the valley floor. These wind speeds were reported to be fairly typical of the

Unauthenticated | Downloaded 11/30/22 12:29 AM UTC

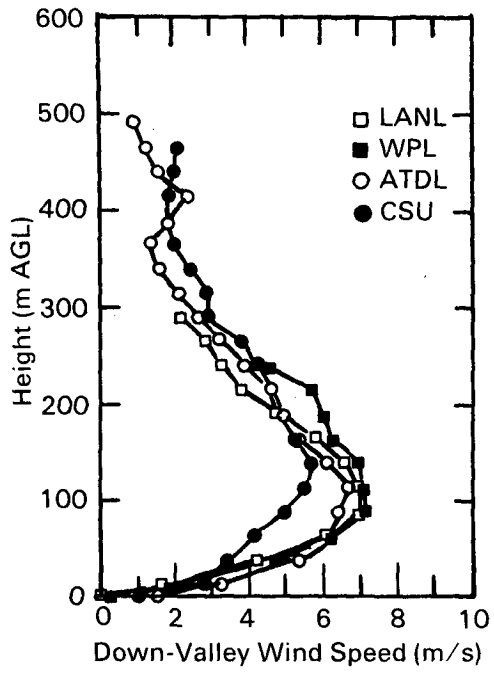

FIG. 4. Average down-valley wind speed as a function of height for four tethered balloon sites.

katabatic wind regime of the Brush Creek Valley under clear skies.

Whiteman and Barr assumed that the valley wind field was uniform across the valley. This assumption was used to calculate mass fluxes on valley cross sections from the available tethered balloon sounding data taken generally from the center of the valley floor. Whiteman and Barr investigated the small amount of wind data available on a cross section of the Brush Valley and concluded that the assumption of cross-valley homogeneity was reasonable in the main part of the valley atmosphere, but that this assumption became invalid as the sidewalls were approached, especially in a zone 150 m above the sidewalls. They estimated that the assumption of horizontal homogeneity caused 15% overestimates of the volume fluxes on a cross section. Recent analyses by ASCOT investigators of Doppler lidar measurements made in the Brush Creek Valley in 1984 (Post and Neff, 1986) suggest that the assumption of cross-valley homogeneity produces volume flux overestimates of 30% to 45%.

In accordance with the model assumptions, we will perform volume flux calculations for the Brush Creek Valley from tethered balloon observations under the assumption of cross-valley homogeneity of the measured wind speed profiles. In a later section of the paper we will discuss the effect on the simulations of overestimates of the volume fluxes caused by this assumption. It should also be mentioned that a series of short tributaries or box canyons are present in the Brush Creek Valley (Fig. 2). Clearly, there will be katabatic flows from the steep tributary canyons injecting negative momentum and thermal energy into the down-valley flow along the main valley. These smaller scale cross-valley transport and mixing processes cannot be explicitly handled in our model; however, the net effect of these smaller scale circulations will be a frictional retardation and cooling of the flow in the main valley. Following arguments by Vergeiner and Dreiseitl (1986) on the role of the slope winds, it will be sufficient for our purposes to consider that the effects of these processes are included in the forcing terms in our momentum and energy equations.

a. The wind field and volume flux

The measured profiles of down-valley wind velocity V at four tethered balloon sites in the Brush Creek Valley (Fig. 4) have been closely fitted analytically in the following way:

$$V = a\zeta e^{-b\zeta}, \tag{9}$$

where the coefficients a and b are functions of the along-valley coordinate ξ [see Eqs. (14) and (15), below]. This means that the height of maximum velocity $\zeta_{max} = 1/b$ also depends on ξ, as is evident from Fig. 4.

Now let the valley width $\Delta y(\xi, \zeta)$ (Fig. 3) also be represented analytically as follows:

$$\Delta y = c(\xi) - d(\xi)e^{-\gamma\zeta}. \tag{10}$$

A good fit to the four stations in Figs. 2 and 3 is obtained by setting

$$c(\xi) = (2.70 + 0.275\xi) \times 10^3 \text{ [m]}, \tag{11}$$

$$d(\xi) = (2.55 + 0.241\,\xi) \times 10^3 \text{ [m]}, \tag{12}$$

where ξ is in kilometers and γ is constant:

$$\gamma = 1.2 \times 10^{-3} [\text{m}^{-1}].$$

With Eqs. (9) and (10), ψ can be evaluated from Eq. (2):

$$\psi(\xi, \zeta) = \frac{ad}{b+\gamma}\left[\zeta e^{-(b+\gamma)\zeta} - \frac{1}{b+\gamma}(1 - e^{-(b+\gamma)\zeta})\right] - \frac{ac}{b}\left[\zeta e^{-b\zeta} - \frac{1}{b}(1 - e^{-b\zeta})\right]. \tag{13}$$

Here, a, b, c and d are functions of ξ. Inserting suitable approximations for $a(\xi)$ and $b(\xi)$, the volume flux ψ increases downstream, as stated by WB, and a sinking motion results in the valley, which, in terrain-following coordinates, is given by

$$w^* = -\frac{1}{\Delta y}\frac{\partial \psi}{\partial \xi},$$

amounting to roughly -10 cm s^{-1} near the rim, which,

Unauthenticated | Downloaded 11/30/22 12:29 AM UTC

again, is within the same order of magnitude as obtained by WB.

However, we need to treat this question a bit more carefully. It is obvious that the downstream increase of volume flux ψ is the net result of two opposing effects: the downstream increase of Δy and, therefore, of the cumulative cross-sectional area [compare Fig. 3 and Eqs. (10), (11), (12)] and the downstream decrease of flow speed V (Fig. 4). Unfortunately, it turns out that the computed vertical velocities, in either terrain-following or $(x$–$z)$-coordinates, and all velocity gradients and other subsequently needed quantities are quite sensitive to small changes of $a(\xi)$ and $b(\xi)$, that is, to the exact way in which the down-valley wind speed V decreases downstream. The functions $a(\xi)$ and $b(\xi)$ that were finally chosen were determined by qualitatively fitting the vertical velocity profiles computed by WB from along-valley wind data and the mass continuity equation. Thus the along-valley and vertical wind velocities are tied to the observed wind data.

All of the various forms of $a(\xi)$ and $b(\xi)$ that were tried produce fields of $V(\xi, \zeta)$ whose differences are small and, in any case, lie well within the fluctuations of the data points. Deviations from stationarity alone leave more than ample leeway for such experiments. To demonstrate this sensitivity, we show in Fig. 5 the fields of flow speed V (in terrain-following coordinates) and the vertical velocity w [in $(x$–$z)$-coordinates] for two choices of a and b.

Case A (final choice):

$$a(\xi) = 0.225 - 0.00442\xi - 0.00096\xi^2 \ [\mathrm{s}^{-1}],$$

$$b(\xi) = (1.12 - 0.00405\xi^2) \times 10^{-2} \ [\mathrm{m}^{-1}],$$

where ξ is expressed in km. (14)

Case B (for comparison):

$$a(\xi) = 0.238 - 0.0134\xi \ [\mathrm{s}^{-1}],$$

$$b(\xi) = (1.18 - 0.0065\xi - 0.0051\xi^2) \times 10^{-2} \ [\mathrm{m}^{-1}],$$

where ξ is in km. (15)

Whereas the fields of down-valley flow V are very similar, the fields of w (and, a fortiori, other derived differentiated quantities not shown in comparison) are substantially different.

From now on, all fields shown and discussed refer to case A [Eq. (14)] only. Also, all subsequent computations are done in the $(x$–$z)$-coordinate frame, in line with the structure of the equations. As $\psi(\xi, \zeta)$ [Eq. (13)] and $\Delta y(\xi, \zeta)$ [Eq. (10)] are given in analytical form, it is a straightforward matter to compute grid-point values of ψ and Δy in the $(x$–$z)$-frame using the coordinate transformations.

Finally, the resulting streamfunction field ψ = cumulative down-valley volume flux is shown in Fig. 6, emphasizing the subsidence that goes along with the downstream increase of volume flux. Just as a check, total volume fluxes up to ridgetop level come out to

Case a: Along-valley wind component, v(m s^{-1})

	Distance (km)				
Height (m)	0	2	4	6	8
600	0.2	0.2	0.2	0.2	0.4
500	0.4	0.4	0.5	0.6	0.9
400	1.0	1.0	1.1	1.3	1.6
300	2.3	2.3	2.4	2.6	2.9
200	4.8	4.7	4.7	4.7	4.6
100	7.3	7.0	6.7	6.2	5.4
0	0.0	0.0	0.0	0.0	0.0

Case b: Along-valley wind component v(m s^{-1})

	Distance (km)				
Height (m)	0	2	4	6	8
600	0.1	0.1	0.2	0.3	0.6
500	0.3	0.3	0.4	0.7	1.2
400	0.8	0.9	1.0	1.4	2.1
300	2.1	2.0	2.2	2.7	3.5
200	4.5	4.3	4.3	4.6	5.3
100	7.3	6.7	6.3	6.1	5.9
0	0.0	0.0	0.0	0.0	0.0

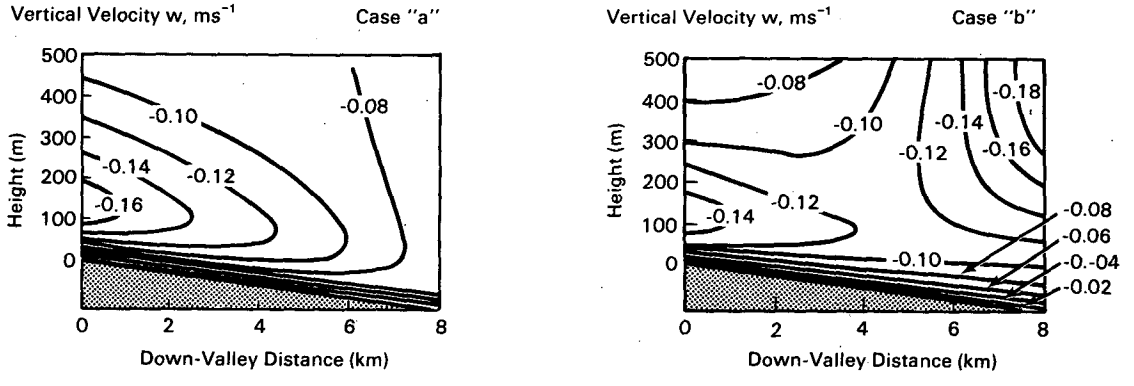

FIG. 5. Comparison of (a) case A [final choice, Eq. (7)] and (b) case B [sensitivity test, Eq. (8)]; horizontal and vertical velocities in m s^{-1}.

Unauthenticated | Downloaded 11/30/22 12:29 AM UTC

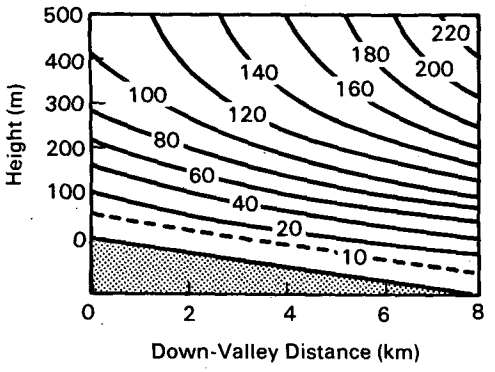

FIG. 6. Streamfunction, ψ, 10^4 m^3 s^{-1}.

be approximately 1.0×10^6 and 2.3×10^6 m^3 s^{-1} at the upstream and downstream ends, respectively (compare WB Fig. 5).

b. *Temperature and pressure*

Information on the nocturnal temperature structure in the valley comes from the 30–31 July 1982 ASCOT dataset. Out of the numerous tethersonde soundings, the 0300 LST soundings were chosen from the five locations available (i.e., LANL, WPL, ATDL, LLNL and CSU), with most emphasis on the LANL and CSU data since they defined the upper and lower ends of the instrumented 8-km segment of the valley. These data show a very strong inversion up to 100 m above the valley floor and a near isothermal stratification from about 150 m upward.

The available soundings indicate a horizontal temperature increase of 3° to 4°C between the upstream and downstream ends of the 8-km-long valley segment under consideration. This corresponds to a 2°C temperature increase along the valley floor. However, the soundings reach, at most, only up to 250 or 350 m above the valley floor, and there are some questions left open, such as the accuracy of intercomparisons between tethered-balloon data collection systems, and the local influence of topography at individual sites. The tethersonde at the CSU site might occasionally be sampling the Roan Creek Valley flow systems. Furthermore, the night of 30–31 July 1982 appears to have a rather large horizontal temperature difference compared to other nights.

In view of the lack of observations at the ridgetop level, we tried various temperature differences, but ended up setting them to 1.5°C near ridgetop level, whereas they are observed to be $\approx$2°C along the valley floor. For convenience, an analytic expression in the $(\xi$–$\zeta)$-frame is used again:

$$T(\xi, \zeta) = T_\infty(\xi) + (T_0(\xi) - T_\infty(\xi))e^{-\delta\zeta}, \qquad (16)$$

where $\delta = 1.30 \times 10^{-2}$ m^{-1}, $T_0(\xi)$ is the temperature along the valley floor, and $T_\infty(\xi)$ is the temperature limit near ridgetop level. Here $T_0(\xi)$ and $T_\infty(\xi)$ are both constructed to fit the data, which show a stronger gradient in the upper, narrower part of the valley, such that

$$\left.\begin{aligned} T_0(\xi) &= T_{01} + \left(1.25\frac{T_{02}-T_{01}}{8\text{ km}}\right)\xi \\ &\quad - \left(0.25\frac{T_{02}-T_{01}}{(8\text{ km})^2}\right)\xi^2 \\ T_\infty(\xi) &= T_{\infty 1} + \left(1.25\frac{T_{\infty 2}-T_{\infty 1}}{8\text{ km}}\right)\xi \\ &\quad - \left(0.25\frac{T_{\infty 2}-T_{\infty 1}}{(8\text{ km})^2}\right)\xi^2 \end{aligned}\right\}, \qquad (17)$$

subscripts 1 and 2 refer to upstream and downstream, and our final choice, as discussed above, is

$$T_{02} - T_{01} = 2°\text{C},$$

$$T_{\infty 2} - T_{\infty 1} = 1.5°\text{C}.$$

Rotation into the $(x$–$z)$-grid is done as before, and the resulting temperature field is shown in Fig. 7.

The pressure deviation field can be obtained from the temperature field by integration using the method outlined in section 2b. The results are shown in Table 1, where we use the $(x$–$z)$-coordinate system with origin at the valley floor at the upper end of the valley segment. Naturally, pressure decreases in the down-valley direction, since the pressure gradient drives the katabatic winds. The total pressure difference along the valley bottom is about 0.3 hPa. This difference seems realistic compared with an estimated pressure difference of about 0.3 hPa along the 15-km-long, 1000-m-deep, but wider Dischma Valley of Switzerland (Egger, 1983). As a consequence of our temperature field structure, horizontal pressure gradients are stronger in the upper, narrower part of the valley. This feature is reasonable in itself, and, as we shall see later, it yields fair agreement between the pressure gradient and advection terms in the momentum balance.

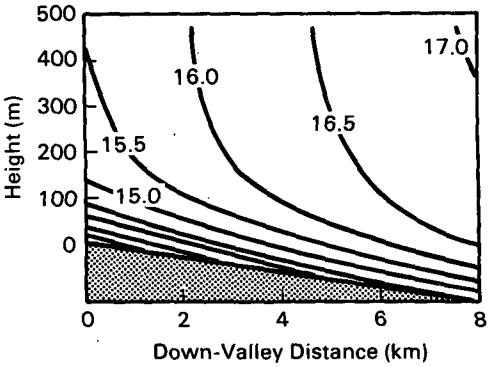

FIG. 7. Temperature field, degrees Celsius.

Unauthenticated | Downloaded 11/30/22 12:29 AM UTC

TABLE 1. Pressure deviation, p', in hPa.

Height (m AGL)	Distance along valley (km) 0	2	4	6	8
480	0.00	0.00	0.00	0.00	0.00
420	0.03	0.02	0.01	0.01	0.00
360	0.06	0.04	0.03	0.01	0.00
300	0.09	0.06	0.04	0.02	0.00
240	0.12	0.08	0.05	0.02	0.00
180	0.15	0.11	0.07	0.03	0.00
120	0.19	0.13	0.08	0.04	0.00
60	0.24	0.16	0.10	0.05	0.00
0	0.30	0.20	0.12	0.06	0.00
−60			0.16	0.07	0.00
−120					0.00

c. *Momentum equation*

The momentum balance for stationary, quasi-two-dimensional flow was given as Eq. (7). The advection and pressure gradient terms in this equation were calculated for the Brush Valley simulation using finite differencing. Table 2 shows the results. The horizontal pressure gradient decreases with height until becoming zero at ridgetop level. The sum of vertical and horizontal momentum advection, as listed in the table, changes sign as the ground is approached. Above the level of the jet, negative fluxes of down-valley momentum are experienced, since the mean subsidence field causes weak down-valley winds to be advected downward into the valley. Below the level of the jet, positive momentum fluxes are experienced as the general subsidence causes downward advection of the strong winds associated with the jet.

TABLE 2. Terms of the momentum equation at different distances along the valley axis.

Height (m AGL)	Distance along valley (km) 1 *	1 †	4 *	4 †	7 *	7 †
480	0.33	0.00	0.24	0.00	0.25	0.00
450	0.43	0.22	0.32	0.18	0.31	0.15
405	0.65	0.55	0.46	0.46	0.42	0.37
360	0.94	0.88	0.66	0.74	0.56	0.60
315	1.30	1.22	0.91	1.02	0.71	0.83
270	1.69	1.57	1.18	1.31	0.86	1.06
225	1.97	1.93	1.42	1.60	0.96	1.29
180	1.90	2.31	1.49	1.91	0.91	1.53
135	1.14	2.74	1.17	2.23	0.61	1.78
90	−0.47	3.26	0.27	2.60	−0.07	2.05
45	−2.09	3.92	−1.11	3.05	−1.11	2.37
0	−2.22	4.84	−1.97	3.63	−2.08	2.75
−45			−1.47	4.46	−2.03	3.25
−90					−0.87	3.99

* Minus momentum advection $\left(u\frac{\partial u}{\partial x}+w\frac{\partial u}{\partial z}\right)$, in 10^{-3} m s^{-2}.

† Pressure gradient $\left(\frac{-1}{\rho}\frac{\partial p'}{\partial x}\right)$, in 10^{-3} m s^{-2}.

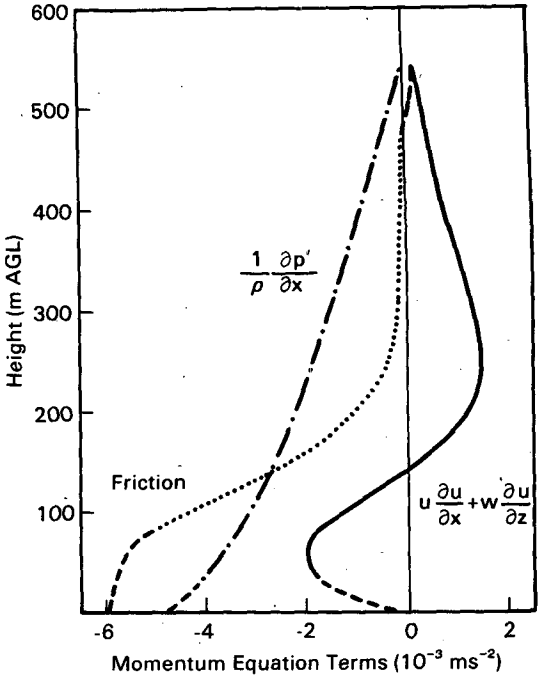

FIG. 8. Terms of the momentum equation at $x = 4$ km, 10^{-3} m s^{-2}.

The balance between all terms of the momentum equation as a function of height at a distance of 4 km down the valley is shown in Fig. 8. Note that this figure is just another way of presenting the center columns (at 4 km) of Table 2. Friction is negative, and the profile makes sense. Regarding its magnitude, we can make an estimate of a Guldberg–Mohn-type linear friction law applied to the first grid point above the valley floor, where the along-valley wind speed is 2.5 m s^{-1}:

$$\text{friction} \approx -5.6\times10^{-3}\,\text{m s}^{-2} = -uk,$$

from which the friction coefficient can be calculated as

$$k \approx \frac{1}{450\text{ s}} \approx \frac{1}{8\text{ min}}.$$

This value seems reasonable compared to reaction times in the much wider Inn Valley of Austria, where they are on the order of 30 min (Vergeiner and Dreiseitl, 1986).

d. *Energy balance equation*

We can next turn our attention to the computation of the terms in the thermal energy balance equation [Eq. (8)]. As we have seen in Fig. 5, a strong subsidence field is present in the valley. Subsidence in the stable valley atmosphere will produce local warming [i.e., $\partial\theta/\partial t = -w(\partial\theta/\partial z)$]. On the other hand, this warming due to subsidence can be counteracted by cold air advection in the down-valley flow. Figure 9 shows the sum of the

Unauthenticated | Downloaded 11/30/22 12:29 AM UTC

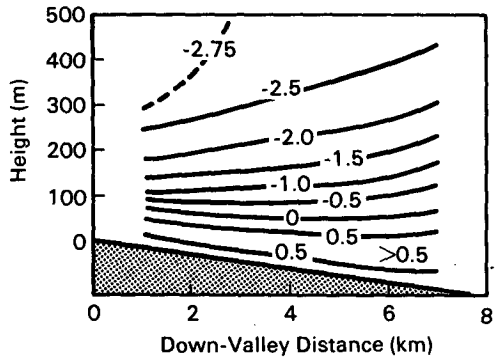

FIG. 9. Minus potential temperature advection, $u(\partial\theta/\partial x) + w(\partial\theta/\partial z)$, degrees Kelvin per hour.

horizontal and vertical potential-temperature advection terms. As we see in the figure, cold air advection by the down-valley wind counteracts the subsidence warming only slightly in the upper levels, but becomes a more important factor in the energy budget in the lower levels of the valley where along-valley winds and horizontal temperature gradients are stronger. There, total temperature advection changes sign, implying that cold air advection overcomes subsidence warming.

If the temperature structure were steady-state, total advection (horizontal + vertical) could be compensated only by diabatic cooling [see Eq. (8)]. In this case, Fig. 9 represents the field of diabatic cooling in the valley. The required maximum diabatic cooling then would be nearly -2.9 K h^{-1}, with the average over the valley being -1.95 K h^{-1}. There is, however, a region of diabatic warming close to the valley floor, with values ranging up to $+0.8$ K h^{-1}. The size of this region of diabatic warming is somewhat overestimated by the fact that we are assuming steady-state conditions. In actuality, the valley atmosphere cooled at an average rate of -0.5 K h^{-1} during the 7-h period. Nonetheless, the location of this region of apparent diabatic warming is reasonable since effective outgoing radiation and sensible heat flux are expected to be reduced on the valley floor relative to the upper sidewalls or mesa tops. This reduction is caused by an increase in the effective radiating temperature of the sky (and thus of downward longwave radiation) as one descends from the sidewalls because of view factor considerations. A second reason for the diabatic warming is the downward mixing of potentially warmer air near the valley floor. Although the air is extremely stably stratified, Richardson numbers are nevertheless below critical values in the lowest dekameters, such that turbulence must occur there. A quantitative estimate shows that an eddy diffusivity of roughly one-fifth the "adiabatic" value (ku^*z from the logarithmic wind profile) would yield the observed warming by turbulent mixing. Again, this warming is plausible considering the strong stability.

In the uppermost layers, warming by subsidence essentially compensates diabatic cooling [Eq. (8)], but horizontal advection $u(\partial\theta/\partial x)$, though minor, changes the numbers somewhat. If we had chosen the temperature difference between the ends of the valley segment at upper levels to be 1°C rather than 1.5°C (our final choice, compare Fig. 7), the diabatic cooling rates needed to establish a balance in Eq. (8) would have increased to -3.5 K h^{-1} (maximum) or -2.4 K h^{-1} (mean), respectively, and the layer of diabatic warming at the bottom would have been shallower. Conversely, increasing the temperature difference near the rim would make the required diabatic cooling rates smaller.

4. Radiative loss and heat balance on the mesa

Our delicate attempts at balancing all equations end up with something qualitatively plausible. We find a weighted mean diabatic cooling rate of roughly -2 K h^{-1} in the valley segment. This diabatic cooling rate would be about -2.5 K h^{-1} if we considered the decrease in energy storage in the valley segment. The diabatic processes of radiative flux convergence and sensible heat flux are responsible for this cooling. To shed more light on the diabatic cooling we wish to consider for the moment that all diabatic cooling comes from surface sensible heat flux. We can then calculate the required mean surface sensible heat flux over the entire area of the valley. The Brush Creek Valley is approximately 25 km long. The core of our calculation is that air is being cooled over the entire catchment area between the two ridge lines (Fig. 2), amounting to approximately 95 km^2, but that this cold air flow is essentially channeled or concentrated into the valley proper below rim height, i.e., the volume we have been concerned with up to now. Taking the whole length of the Brush Creek Valley, a mean cross-sectional area up to the rim would be 0.40×10^6 m^2 (near the upstream station listed in WB; see their Fig. 1), as opposed to a mean cross section of approximately 0.68×10^6 m^2 for the 8-km segment at the lower end of the entire valley. Now, let the mean sensible heat flux, to be estimated, be $\bar{H}$ [W m^{-2}], positive upward.

From the first law of thermodynamics

$$\bar{H} \times 95\,[\mathrm{km}^2] = \rho c_p \frac{\delta \bar{T}}{\delta t} \times 0.40 \times 10^6\,[\mathrm{m}^2] \times 25\,[\mathrm{km}].$$

$$\begin{matrix}\text{sensible heat withdrawn} \\ \text{from the air and/or} \\ \text{radiative flux divergence}\end{matrix} = \begin{matrix}\text{change of} \\ \text{heat content} \times \\ \text{per volume}\end{matrix} \begin{matrix}\text{volume} \\ \text{of} \\ \text{valley}\end{matrix} \qquad (18)$$

Taking the "observed" value for diabatic heating of approximately -2 K h^{-1} for $\delta\bar{T}/\delta t$, it follows from (18) that $\bar{H} = -58$ W m^{-2}. This energy has to be withdrawn, on the average, from the air close to the ground. The corresponding number for -2.5 K h^{-1} is $\bar{H} = -73$ W m^{-2}.

We can do similar calculations for the 8-km valley segment using a catchment area of 32.5 km^2 and a

Unauthenticated | Downloaded 11/30/22 12:29 AM UTC

mean cross-sectional area of 0.68×10^6 m^2. For a diabatic cooling rate of -2 K h^{-1} this calculation results in a mean sensible heat flux of -92 W m^{-2}; for a cooling rate of -2.5 K h^{-1} we get -116 W m^{-2}.

There are no energy balance data available for the night of 30–31 July, but preliminary results from ASCOT measurements in the same valley in 1984 show effective outgoing radiation values of up to -70 W m^{-2} (Simpson et al., 1985). However, preliminary analyses of this data show that soil heat flux largely counteracts this net radiation deficit. Evaporation rather than condensation typically occurs at night in the semiarid Brush Creek Valley climate. This latter fact would actually boost the (negative) sensible heat flux from the air a bit, but our best estimate of surface sensible heat flux from preliminary observations taken in the Brush Creek Valley in the fall of 1984 is only approximately -25 W m^{-2}, considerably short of what is required. On the other hand, we find nocturnal sensible heat fluxes reaching -80 W m^{-2} in the literature for comparable sites (Staudinger, 1983; Rott, 1979), and heat budgets could vary considerably between summer 1982 and fall 1984, depending on soil conditions, wind, humidity and other factors.

As a last resort, we could postulate that radiative flux divergence makes up the difference. In principle, longwave-radiation flux divergences act to cool the atmosphere, and cooling is concentrated in the lower layers. However, we will not pursue this notoriously unknown quantity any further here. We remark in concluding that there are two ways to alleviate the rather large diabatic cooling requirement.

1) As mentioned previously, the wind field we use (Figs. 4 and 5) could be overestimated by up to 45%. Correspondingly, u, w and temperature advection would be reduced proportionately in amount, and likewise the required diabatic cooling.

2) If the horizontal temperature difference near the rim is larger than 1.5°C (see the discussion at the end of section 3d), we need less cooling for balance. Larger horizontal temperature gradients are, in fact, quite compatible with our data.

5. Conclusions

A method was proposed to evaluate the coupled mass, momentum and thermal energy budget equations for a deep valley under nocturnal, two-dimensional, steady-state flow conditions. The method requires the temperature, down-valley wind and valley width fields to be approximated on a two-dimensional vertical grid that runs down the valley axis. Advection terms in the momentum and energy equations are then calculated using finite differences computed on the grid. The pressure gradient term in the momentum equation is calculated from the temperature field by means of the hydrostatic equation. The friction term is then calculated as a residual in the x-momentum equation, and the diabatic cooling term is calculated as a residual in the thermal energy budget equation.

Using this method, the dynamics of the katabatic circulation system in the deep, narrow Brush Creek Valley of Colorado were evaluated during a time of steady-state nocturnal drainage flows. The evaluation was accomplished using simple analytical functions to describe the vertical and along-valley structure of the wind and temperature fields and the valley width. A key assumption was that the wind and temperature fields were uniform across the valley. The analytical functions were fit to data collected by four tethered-balloon data collection sytems operated at different points along the axis of the valley in the lowest 8-km segment of the valley during the night of 30–31 July 1982. Individual terms of the budgets were computed on a numerical grid using finite differences or were calculated as residuals.

Tethered balloon observations in the valley taken during a quasi-steady-state period from 2200 to 0500 LST showed down-valley winds in the valley with peak speeds of 7–8 m s^{-1} in a jet axis located only 90–150 m above the valley floor. The height of the jet increased slightly and the peak speeds decreased slightly with down-valley distance. The valley's temperature field was characterized by an intense but shallow inversion in the lowest 100 m above the valley floor. This intense inversion was surmounted by an isothermal temperature layer that extended from 150 m through the remaining valley depth.

The mass budget of the valley was investigated by deriving a streamfunction in which the numerical values represent the cumulative along-valley volume flux up to the height of integration. The computed volume or mass fluxes depend on the product of valley width and along-valley wind speed component. The large relative increase in valley width in the valley segment investigated resulted in volume fluxes that increased strongly with down-valley distance. Volume fluxes increased from 1 million to 2.3 million m^3 s^{-1} from the upstream to the downstream ends of the valley segment. Calculations showed that this increase in down-valley volume flux, if supported solely by subsidence in the valley atmosphere, would result in peak subsidence rates of about 0.10 m s^{-1} with subsidence generally through the entire valley depth.

Tethered balloon observations showed that temperatures increased on horizontal surfaces from the upstream to downstream ends of the valley segment. Temperature increases were about 2°C along the valley floor in the lower levels of the atmosphere and were assumed to be 1.5°C near ridgetop levels. Because of this temperature field structure, down-valley winds produced cold air advection, as expected. Hydrostatic calculations estimated that maximum horizontal pressure gradients were 0.3 hPa/8 km at the ground near the upstream end of the valley segment.

The along-valley momentum budget under steady-

Unauthenticated | Downloaded 11/30/22 12:29 AM UTC

state conditions requires a balance among vertical and horizontal momentum advection, the pressure gradient force, and the force of friction. An example of the vertical variation of individual terms in the momentum equation was provided for a location near the middle of the valley segment. Subsiding motions in the valley produced negative vertical down-valley momentum fluxes in the upper valley atmosphere, but produced positive down-valley momentum fluxes below the level of the jet. Friction, calculated as a residual in the x-momentum equation, was negative, as expected on physical grounds, and attained reasonable quantitative values. It was nearly zero in the upper part of the valley atmosphere but increased in the lowest 200 m to a maximum value of -0.006 m s^{-2} as the ground was approached.

The thermodynamic energy equation requires a balance among the change in heat storage in the valley, vertical and along-valley advection of potential temperature, and diabatic heating. Change in heat storage in the valley segment was at the rate of about -0.4 K h^{-1} when integrated over the valley volume. The strong subsidence field in the stable valley atmosphere produced subsidence warming ($+2.5$ K h^{-1}) that was only partly counteracted by down-valley cold air advection (-0.5 K h^{-1}). Strong diabatic cooling (-2.0 K h^{-1}) was required to balance the thermal energy budget equation. This large rate of diabatic cooling seems somewhat too large to be supplied by the diabatic processes of sensible heat flux and radiative flux divergence. No information on these processes is available for the 1982 ASCOT experiments, but sensible heat flux measurement made by several investigators in the Brush Creek Valley in 1984 should be available soon.

Recent observational evidence suggests that the cross-valley homogeneity assumption used in the calculations significantly overestimates along-valley volume flux divergence and, thus, the rates of subsidence and subsidence heating. The excessive diabatic cooling requirement appears to be caused by the large rate of subsidence heating. Thus, diabatic cooling would be significantly reduced by more realistically accounting for the cross-valley structure of the down-valley wind system.

Acknowledgments. The authors wish to thank Mr. R. Kloetzer of the University of Innsbruck for computer programming assistance. Tethered balloon soundings used in the analysis were collected by participants in the U.S. Department of Energy's ASCOT program. C. D. Whiteman's contribution to the work was supported by the North Atlantic Treaty Organization under a grant awarded in 1983 and, in part, by the U.S. Department of Energy under Contract DE-AC06-76RL0 1830 at Pacific Northwest Laboratory. Pacific Northwest Laboratory is operated for the U.S. Department of Energy by Battelle Memorial Institute.

REFERENCES

Egger, J., 1983: Pressure distribution in the Dischma valley during the field experiment DISKUS. *Beitr. Phys. Atmos.*, **56**(2), 163–176.

Post, M. J., and W. D. Neff, 1986: Doppler lidar measurements of winds in a narrow mountain valley. *Bull. Amer. Meteor. Soc.*, **67**, 274–281.

Rott, H., 1979: Vergleichende Untersuchungen der Energiebilanz im Hochgebirge (Comparative studies of the energy balance in high mountains). *Arch. Meteor. Geophys. Bioklim.*, **A28**, 211–232.

Simpson, J. R., L. J. Fritschen, C. D. Whiteman and M. M. Orgill, 1985: Energy balance in a deep Colorado valley: ASCOT84. *Preprints 17th Conf. on Agriculture and Forest Meteorology*, Phoenix, Amer. Meteor. Soc., 8–11.

Staudinger, M., 1983: Der Waermehaüshalt zweier hochalpiner Stationen waehrend der Vegetationsperiode (The energy budget of two high mountain stations during the vegetation season). Thesis, Universitaet Innsbruck, 245 pp.

Vergeiner, I., and E. Dreiseitl, 1987: Valley winds and slope winds; observations and elementary thoughts. *Meteor. Atmos. Phys.* (special ALPEX issue), (in press).

Whiteman, C. D., and S. Barr, 1986: Atmospheric mass transport by along-valley wind systems in a deep Colorado valley. *J. Climate Appl. Meteor.*, **25**, 1205–1212.

Unauthenticated | Downloaded 11/30/22 12:29 AM UTC